Universal Readout System for Temperature, Elongation and Hydrostatic Pressure Sensors Based on Highly Birefringent Fibers

W. J. Bock, *Senior Member, IEEE*, M. S. Nawrocka, and W. Urbanczyk

***Abstract*—In this paper, we present a universal readout system, which can be used to decode polarimetric fiber-optic sensors based on highly birefringent fibers. All such sensors use the same sensing principle, relying upon the dependence of modal birefringence on different physical parameters. To register the measurand-induced phase changes between polarization modes, we use the coherence-addressing principle. This requires that the interrogated sensor be powered by a broadband source (superluminescent diode) and that the total optical path delay introduced by the sensor be balanced in the decoding interferometer. The system performance in decoding elongation, temperature and hydrostatic pressure sensing is demonstrated.**

***Index Terms*—Coherence-multiplexing, fiber-optic sensor, measurement of pressure, temperature and elongation.**

I. Introduction

THE fundamental problem associated with interferometric sensors is the loss of clarity in phase-shift recovery when the sinusoidal intensity exceeds extreme values, thereby limiting the measuring range to 180°. Numerous efforts have been directed to eliminating this problem and to making the response of interferometric sensors linear in a wide range of phase shifts. The basic idea is to create two interferometric signals at the sensor output that are proportional to $\sin\phi$ and $\cos\phi$, where ϕ is a phase shift introduced by the measurand [1]–[5].

The demodulation method described in this paper employs a low-coherence interferometric principle. This principle requires that the sensing and receiving interferometers be arranged in tandem. Each of the interferometers has an optical path delay (OPD) greater than the coherence length of the source, while the difference of their OPDs is less than the coherence length of the source. If these conditions are fulfilled, a differential interference signal associated with both interferometers is observed at the output of the receiving interferometer. The decoding interferometer is composed of four detection channels. Each channel contains crystalline-quartz plates, which compensate the OPD that is introduced by the interrogated sensor. The fading problem is solved by tilting the quartz plates, thereby introducing an initial phase shift equal to 45° between consecutive interference signals. This makes it possible to measure the phase shift with a resolution of 1/8 of the interference fringe in a range of about 60 fringes. This range is limited only by the coherence length of the source.

The proposed detection method is simple and inexpensive. In contrast to the recently proposed two-wavelength technique [4], [5], the phase differences between signals generated in different detection channels remain the same throughout the whole measurement range. The proposed method is suitable only for measurements of relative changes of the phase shift. The method also makes it possible to recognize the direction of the changes of the phase shift. The system can be applied to decoding any fiber-optic sensor based on highly birefringent fibers.

Manuscript received March 1, 2003; revised September 25, 2003. This work was supported in part by the Natural Sciences and Engineering Research Council of Canada and in part by the Polish Committee for Scientific Research under Grant 8T10C 020 18.

W. J. Bock and M. S. Nawrocka are with the Centre de recherche en photonique, Département d'informatique et d'ingénierie, Université du Québec en Outauais, Gatineau, Québec, QC J8X 3X7 Canada (e-mail: bock@uqo.ca).

W. Urbanczyk is with the Institute of Physics, Wroclaw University of Technology, Wroclaw, Poland (e-mail: urban@if.pwr.wroc.pl).

Digital Object Identifier 10.1109/TIM.2003.822193

II. Construction of the Decoding System

The decoding system is equipped with a superluminescent diode from Anritsu, Ltd., pigtailed with 3M polarizing fiber, as shown in Fig. 1. Linearly polarized light from the polarizing fiber is coupled by a polarization maintaining connector into one mode of the linking fiber (Corning PMF-38). The linking fiber and the active part of the sensor are spliced to each other with rotation of their polarization axes by $\alpha_1 = 45°$. Therefore, two polarization modes are excited in the active elements of the sensor. The output of the sensor is spliced to a lead-out fiber with rotation of their polarization axes by $\alpha_3 = 45°$. The output of the lead-out fiber is aligned $\alpha_4 = 45°$ with respect to the polarization axes of the crystalline-quartz delay plate. These rotations assure the maximum contrast of the interference signal at the detection channels [6], [7].

The detection system is composed of four channels for registering interference signals and one channel for measuring the average intensity at the sensor output. The interference phenomenon can be observed at the detection channels only if the total optical path delay ΔR_S introduced by the interrogated sensor is compensated by the optical path delay ΔR_Q introduced by the compensating quartz plates. The plates can be tilted with respect to the incident beam in order to make the initial phase shift of the interference signal different in every decoding channel. The intensity registered in the i-th detection channel may be represented by the following equation:

$$I_i = I_0\left[1 + 0.5\gamma\left(\Delta R_S - \Delta R_Q^i\right)\sin\left(\Delta\phi_S - \Delta\phi_Q^i\right)\right] \quad \mathrm{i} = 1,2,3,4. \tag{1}$$

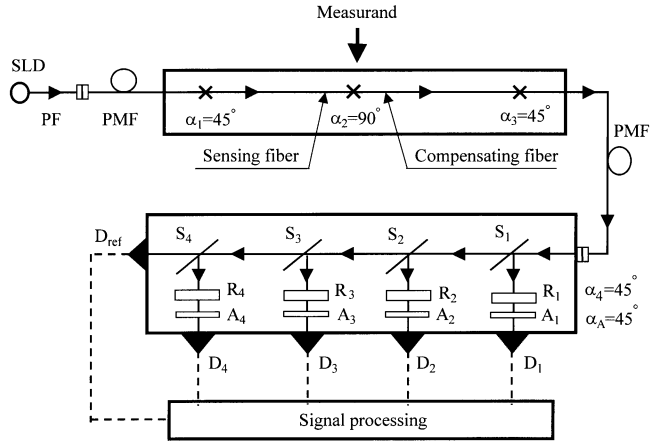

Fig. 1. Scheme of the interferometric system for decoding sensors based on highly birefringent fibers. SLD: superluminescent diode, PF: polarizing fiber, PMF: polarization maintaining fiber, S_1, S_2, S_3, S_4: beam splitters, R_1, R_2, R_3, R_4: crystalline_quartz delay plates, A_1, A_2, A_3, A_4: analyzers, D_1, D_2, D_3, and D_4, D_{ref}: pin photodiodes.

Here I_0 is the average intensity monitored by the reference detector, and γ is the contrast function associated with the source spectrum. The phase shifts $\Delta\phi_Q^i$ introduced by the quartz plates in successive channels differ by 45°, which corresponds to 1/8 of an interference fringe. At the same time, the contrast of all interference signals remains practically the same because γ is a slowly changing function of OPD imbalance $(\Delta R_S - \Delta R_Q)$ compared to the fast intensity variations associated with interference fringes. Sinusoidal intensity changes registered in the detection channels are converted into digital signals in such a way that a high level is generated when the interference signal is greater than the average intensity I_0. A low level is generated for $I_i < I_0$. This makes it possible to measure fast phase shifts induced by an external parameter acting on the sensing element with a resolution of 1/8 of an interference fringe. This also allows for easy recognition of the direction of phase changes.

In the proposed decoding method, the measuring range of the system is limited by the spectral width of the source. Assuming a Gaussian shape of the source spectrum, we can describe the degradation of the contrast with the increasing imbalance of OPD between the sensing and receiving interferometers in the following way:

$$\gamma = \exp\left[-\left(\frac{\pi\delta\lambda}{2\sqrt{2}\lambda_0}\frac{\Delta R_S - \Delta R_Q}{\lambda_0}\right)^2\right] \tag{2}$$

Here, $\delta\lambda$ is the full spectral width at half the maximum of the Gaussian distribution, and λ_0 is a central wavelength of the source. For proper operation of the electronic unit producing the digital pulses, the amplitude of the interference signal must be greater than 10% of the average intensity.

This requirement is equivalent to the following condition:

$$|\Delta R_S - \Delta R_Q| < \frac{2.53\sqrt{2}{\lambda_0}^2}{\pi\delta\lambda}. \tag{3}$$

The OPD introduced by the sensor between x- and y-polarized modes may be represented as

$$\Delta R_S = \Delta R_S^0 + \Delta R_S^X. \tag{4}$$

Here, ΔR_S^0 is the initial OPD (for $X = 0$), and ΔR_S^X is an additional OPD induced by the applied measurand. Depending on the sign of ΔR_S^X, the initial alignment of the system should satisfy one of the following conditions:

$$\Delta R_S^0 - \Delta R_Q = \pm\frac{2.53\sqrt{2}\lambda_0^2}{\pi\,\delta\lambda} \tag{5}$$

respectively for negative and positive ΔR_S^X, as in Fig. 2. It is no problem to fulfill the above condition with an accuracy of $2\,\lambda_0$. The beat length of highly birefringent fibers is typically about 1.5 mm, and the length of the sensing fibers may be easily controlled with a precision of 3 mm. If the above condition is satisfied, the full range of the system is limited by the spectral linewidth of the source and may be expressed by the following equation:

$$\Delta R_{S\max}^X = \frac{5.06\sqrt{2}{\lambda_0}^2}{\pi\,\delta\lambda}. \tag{6}$$

For the superluminescent diode presently used, $\lambda_0 = 849$ nm and $\delta\lambda = 17$ nm. The theoretical operating range according to the above equation is equal to 112 interference fringes ($\Delta R_{S\max}^X = 112\ \lambda_0$). In practice, however, a range of 60 fringes (about 500 counts) was achieved. This is due to contrast degradation caused by imperfect angular alignment of successive sensor elements ($\pm 5°$) and by polarization changes introduced by the beam splitters.

III. Sensor Construction and Performance

Highly birefringent fibers are sensitive to various physical parameters such as hydrostatic pressure, elongation, and temperature. The result is that fiber-optic pressure and elongation sensors based on this type of fiber have to be compensated for temperature. Most often, a reference fiber located as close as possible to the sensing fiber is used to assure temperature compensation [8].

We adopted this concept in building the temperature-compensated sensor for measuring elongation. As shown in Fig. 3(a), it is composed of sensing ($L_S = 0.980$ m) and compensating fibers ($L_C = 0.960$ m) spliced together with rotation of their polarization axes by 90°. A small difference in length (about 2 cm) between the sensing and compensating fibers assures ΔR_S^0 of about 15 λ_0. This is a necessary condition for coherency readout. This residual length difference compromises the temperature stability of the sensors to the level of 0.1 rad/K. In order to calibrate the sensor, we stretched part of the sensing fiber ($L_0 = 0.750$ m) to the maximum strain, equal to 2.63 mstrain [see Fig. 3(b)]. The sensor resolution was estimated at 8.5 μstrain. Furthermore, we observed no hysteresis effect, even after numerous cycles of stretching the sensing fiber. To demonstrate the system response to dynamic strain changes, we glued the sensing fiber to the metal beam. The metal beam was then excited to oscillations. The response of the sensors to decaying oscillations is shown in Fig. 3(c), (d). In these tests, we also established that the maximum counting speed of the decoding system is 10 kHz. This speed is limited by the computer board for data acquisition.

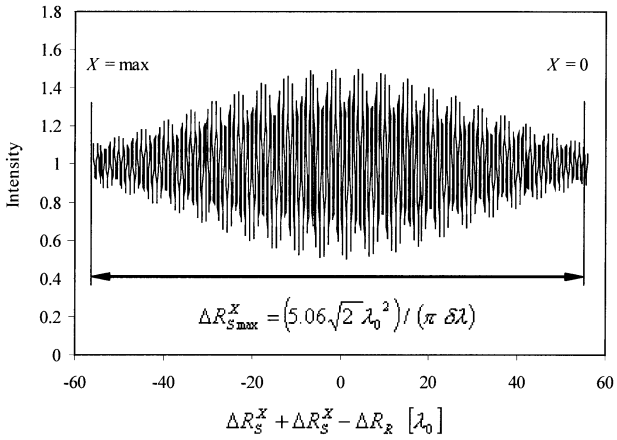

Fig. 2. Optimal adjustment of the initial group retardation of the sensor, in which applied measurand X causes decrease of the optical path delay.

The temperature sensor is composed of Fibercore HB 800 fiber with stress-induced birefringence ($\mathrm{L_S} = 1.020$ m) and of Corning PMF-38 fiber with elliptical core ($\mathrm{L_C} = 0.775$ m), spliced in a differential configuration [see Fig. 4(a)]. It is well known that fibers with stress-induced birefringence are much more sensitive to temperature ($\mathrm{K_{BT}^T} = -4.5$ rad/K m) than elliptical core fibers ($\mathrm{K_{EC}^T} = -0.7$ rad/K m). Through differential configuration with this choice of fibers for temperature sensors, it is easy to assure the proper OPD of the sensor ($65\ \lambda_0$) while only slightly diminishing the sensor response to temperature. Furthermore, by changing the length of these two fibers, we can easily modify the measuring range of the sensor. To make the sensor more compact, the two fibers were wound in a coil about 5 cm in diameter and placed in the sensor housing. The sensor was calibrated against a Haake temperature stabilizer, which is able to control temperature with a precision of 0.1 °C. In Fig. 4(b), the sensor response to step-like temperature changes from 5 °C to 75 °C is presented. During the time when temperature is increasing or decreasing, the sensor readings for the same values of temperature remain identical within the sensor resolution. This shows that no hysteresis occurs. Based on this measurement, we determined the calibration curve, which is shown in Fig. 4(c). The described sensor construction assures an operating range of 70 °C and resolution of 0.2 °C. A similar sensor was initially applied to temperature measurements on a dielectric heat pipe in the presence of high voltage [10]. The described results show promising capabilities of the fiber optic sensors for the measurements where well-known electric sensors cannot be used due to the occurrence of high electromagnetic interference. However, the temperature sensors as well as strain sensors should be further tested with respect to their statistical repeatability. This testing will contribute to improving their measurement accuracy.

In the pressure sensor, the sensing and compensating fibers are located in the same compartment of the sensor head. This assures better temperature compensation in dynamic pressure measurements [see Fig. 5(a)]. This configuration was implemented by applying the side-hole fiber as a sensing element ($\mathrm{L_S} = 1.150$ m) and the elliptical core fiber as a temperature compensating element ($\mathrm{L_C} = 1.380$ m). Due to the different signs of pressure sensitivity of the side-hole and

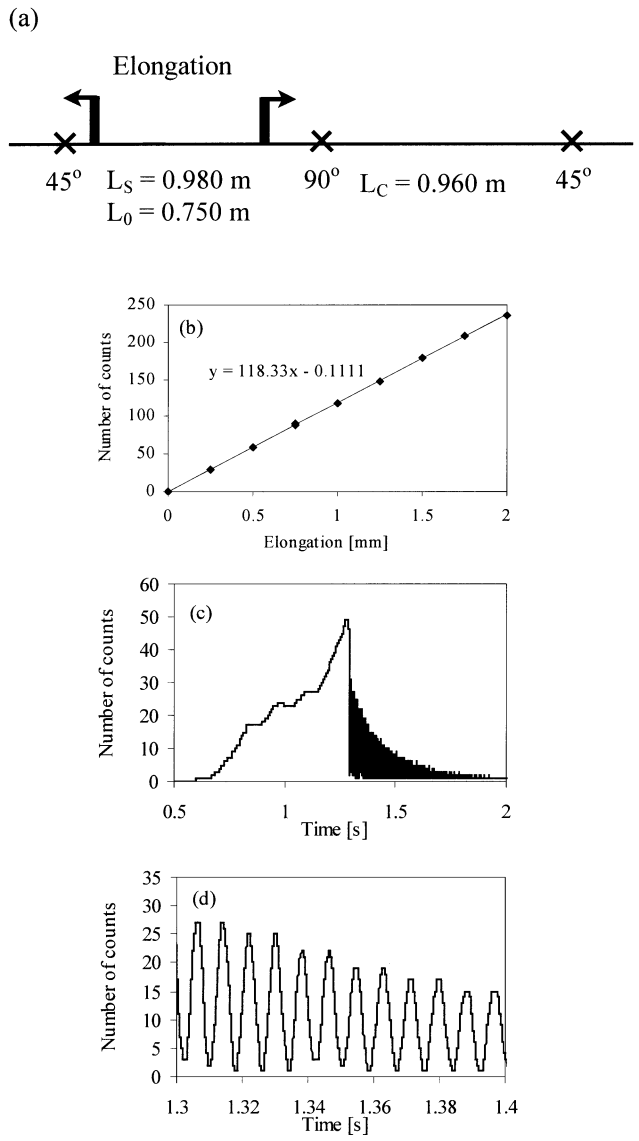

Fig. 3. (a) Construction of the strain sensor, (b) its calibration curve, and (c) response to dynamic strain changes with (d) enlarged part showing the oscillations.

elliptical core fibers (respectively $\mathrm{K_{SH}^P} = -94$ rad/MPa m and $\mathrm{K_{EC}^P} = 0.5$ rad/MPa m), the overall phase shift induced by pressure is enhanced in the proposed configuration. At the same time, the response of such a sensor to temperature can be reduced to almost null (0.02 rad/K) by making the lengths of these two elements inversely proportional to their temperature sensitivities ($\mathrm{K_{SH}^T} = -0.47$ rad/K m and $\mathrm{K_{EC}^T} = -0.39$ rad/K m). The detailed characteristics of this type of sensor may be found in [9]. In Fig. 5(b) the sensor response to step-like pressure changes from 0 to 2.1 MPa is presented. In Fig. 5(c) the calibration curve is presented. This analysis made it possible to establish that the measurement resolution of the pressure sensor is equal to 7.5 kPa. Additionally, an example of the sensor response to fast pressure changes from 0 to 2.1 MPa is shown in Fig. 5(d). We tested nine pressure sensors composed of different fibers (side-hole, bow-tie and elliptical-core) with differential [8] and minimized temperature compensation [11]. All the sensors show very good

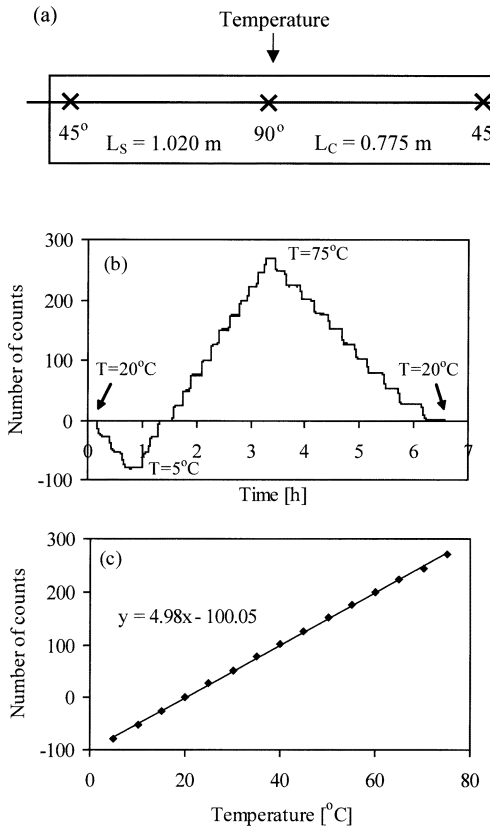

Fig. 4. (a) Construction of the temperature sensor, (b) its response to step-like ($\Delta T = 5$ °C) temperature changes, and (c) the calibration curve.

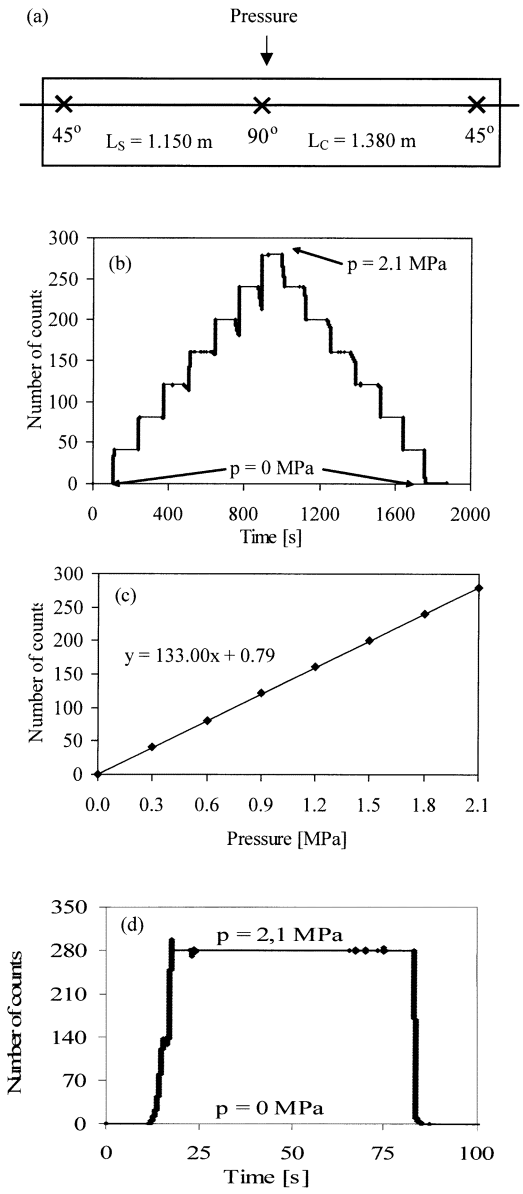

Fig. 5. (a) Construction of the pressure sensor, (b) its response to step-like ($\Delta p = 0.3$ MPa) pressure changes in a range of 2.1 MPa, (c) calibration curve, and (d) example of fast pressure changes from 0 to 2.1 MPa.

linearity, characterized by correlation coefficients from 0.9999 to 1. Taking into consideration the cross-sensitivity effect [12], [13], the maximum change of pressure sensitivity is equal to 0.7% of the average pressure sensitivity within the temperature range of 40 °C. Based on these measurements we conclude that the demodulation system shows good repeatability of phase shift measurements. The evaluated maximum uncertainty of the digital decoding system is equal to 0.4% of full scale.

IV. Summary

In this paper, we presented a universal readout system for decoding polarimetric sensors based on highly birefringent fibers. We have shown that with alteration of sensor construction and the type of sensing fibers, such sensors can be applied in the measurement of different physical parameters, such as elongation, temperature, and hydrostatic pressure. The presented devices have a maximum counting speed of 10 kHz and a resolution of 8.5 μstrain, 0.2 °C, and 7.5 kPa, respectively, for strain, temperature, and pressure measurements. It should be stressed, however, that the characteristics of the sensors can be varied in a wide range simply by changing the lengths of the sensing and compensating fibers. The operating range of the detection system is limited by the width of the spectral characteristic of the light source.

Theoretical analysis shows that the system operating range should be about 1000 counts for the light source presently used. However, the range actually achieved is only 500 counts. This is due to the low precision of angular alignment of successive sensor elements. This precision has to be further improved to increase the performance of the decoding unit, according to the results of the numerical optimization described in [14].

References

[1] S. K. Sheem, "Optical fiber interferometers with [3 × 3] directional couplers: analysis," *J. Appl. Phys.*, vol. 52, pp. 3865–3872, 1981.

[2] S. K. Sheem, T. G. Giallorenzi, and K. Koo, "Optical techniques to solve the signal fading problem in fiber interferometers," *Appl. Opt.*, vol. 21, pp. 689–693, 1982.

[3] R. D. Turner, D. G. Laurin, and R. M. Measures, "Localized dual-wavelength fiber-optic polarimeter for the measurement of structural strain and orientation," *Appl. Opt.*, vol. 31, pp. 2994–3003, 1992.

[4] N. Furstenau, M. Schmidt, W. J. Bock, and W. Urbanczyk, "Dynamic pressure sensing with a fiber-optic polarimetric pressure transducer with two wavelength passive quadrature readout," *Appl. Opt.*, vol. 37, pp. 663–671, Feb. 1998.

[5] A. Ezbiri and R. P. Tatam, "Passive signal processing for a miniature Fabry-Perot interferometric sensor with a multimode laser diode source," *Opt. Lett.*, vol. 20, pp. 1818–1820, 1995.

[6] W. Urbanczyk, P. Kurzynowski, W. A. Wozniak, and W. J. Bock, "Performance analysis of a tandem of white-light fiber-optic interferometers," *Opt. Commun.*, vol. 135, pp. 1–6, Feb. 1997.
[7] W. A. Wozniak, P. Kurzynowski, W. Urbanczyk, and W. J. Bock, "Contrast analysis for a fiber-optic white-light interferometric system," *Appl. Opt.*, vol. 36, pp. 8862–8870, Dec. 1997.
[8] J. P. Dakin and C. A. Wade, "Compensated polarimetric sensor using polarization-maintaining fiber in a differential configuration," *Electron. Lett.*, vol. 20, pp. 51–53, 1984.
[9] W. Urbanczyk, M. S. Nawrocka, and W. J. Bock, "Digital demodulation system for low-coherence interferometric sensors based on highly birefringent fibers," *Appl. Opt.*, vol. 40, pp. 6618–6625, Dec. 2001.
[10] A. Bryszewska-Mazurek, T. Martynkien, W. Mazurek, and J. Rutkowski, "Temperature measurements on a surface of a dielectric heat pipe," *Elect. Eng. Rev. 78*, vol. 10, pp. 30–33, 2002.
[11] W. J. Bock, M. S. Nawrocka, and W. Urbanczyk, "Studies of temperature-insensitive dynamic pressure sensing using elliptical-core side-hole fibers," in *Proc. Int. Conf. Applications on Photonic Technology*, Montreal, QC, Canada, May 25–29, 2003.
[12] W. J. Bock and W. Urbanczyk, "Temperature-hydrostatic pressure cross-sensitivity effect in elliptical-core highly birefringent fibers," *Appl. Opt.*, vol. 35, pp. 6267–6270, 1996.
[13] ——, "Cross-sensitivity effect in temperature-compensated sensors based on highly birefringent fibers," *Appl. Opt.*, vol. 33, pp. 6078–6083, 1994.
[14] M. S. Nawrocka and W. Urbanczyk, "Optimization of detection system for low-coherence interferometric sensors based on highly birefringent fibers," *Opt. Appl.*, vol. 31, pp. 231–250, 2001.

W. J. Bock (SM'90), photograph and biography not available at the time of publication.

M. S. Nawrocka, photograph and biography not available at the time of publication.

W. Urbanczyk, photograph and biography not available at the time of publication.